This document was prepared in conjunction with work accomplished under Contract No. DE-AC09-96SR18500 with the U.S. Department of Energy.

Proceedings of ICAPP 2007
Nice, France, May 13-18, 2007
Paper 7138

Effect of Electrolyzer Configuration and Performance on Hybrid Sulfur Process Net Thermal Efficiency

Maximilian B. Gorensek
Savannah River National Laboratory
Computational and Statistical Science Department
Aiken, SC 29808 USA
Tel: 803.725.1314, Fax: 803.725.8829, Email: maximilian.gorensek@srnl.doe.gov

Abstract – *The Hybrid Sulfur cycle is gaining popularity as a possible means for massive production of hydrogen from nuclear energy. Several different ways of carrying out the SO_2-depolarized electrolysis step are being pursued by a number of researchers. These alternatives are evaluated with complete flowsheet simulations and on a common design basis using Aspen Plus™. Sensitivity analyses are performed to assess the performance potential of each configuration, and the flowsheets are optimized for energy recovery. Net thermal efficiencies are calculated for the best set of operating conditions for each flowsheet and the results compared. This will help focus attention on the most promising electrolysis alternatives. The sensitivity analyses should also help identify those features that offer the greatest potential for improvement.*

I. INTRODUCTION

Interest in the Hybrid Sulfur (HyS) cycle as a means of producing hydrogen (H_2) from nuclear energy on a massive scale has been steadily growing. While the Sulfur-Iodine (SI) cycle has been the subject of the majority of thermochemical H_2 production R&D in recent years, the HyS cycle has also benefited from this investment. For example, both HyS and SI include a high-temperature sulfuric acid (H_2SO_4) decomposition step that produces oxygen (O_2), sulfur dioxide (SO_2), and water (H_2O), so advances in this technology can be applied to both cycles.

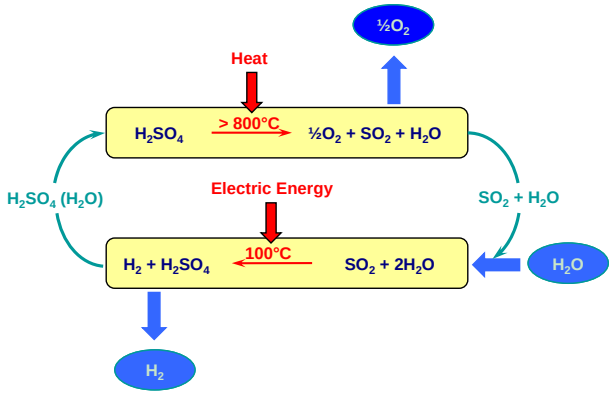

Fig. 1. The Hybrid Sulfur cycle

The two cycles differ, however, in the way in which SO_2 is oxidized to H_2SO_4 and H_2O is reduced to H_2.

The HyS cycle couples the oxidation of SO_2 with the splitting of H_2O and reduction of the resulting protons (H^+) in a single, electrochemical (hence the origin of the "hybrid" designation) step – SO_2-depolarized electrolysis. This is illustrated in Fig. 1 above.

What makes HyS viable is that SO_2-depolarized electrolysis can be carried out at cell potentials much smaller than those for H_2O electrolysis. The standard cell potential for electrolyzing H_2O,

$$\begin{aligned}&\text{Anode: } H_2O\,(l) \rightarrow \tfrac{1}{2}\,O_2\,(g) + 2\,H^+\,(aq) + 2\,e^-, \quad E° = -1.229\text{ V}\\ &\text{Cathode: } 2\,H^+\,(aq) + 2\,e^- \rightarrow H_2\,(g), \quad E° = 0.0\text{ V}\\ &\text{Overall: } H_2O\,(l) \rightarrow H_2\,(g) + \tfrac{1}{2}\,O_2\,(g), \quad E° = -1.229\text{ V}\end{aligned} \qquad (1)$$

is −1.229 V, while that for SO_2-depolarized electrolysis,

$$\begin{aligned}&\text{Anode: } 2\,H_2O\,(l) + SO_2\,(aq) \rightarrow H_2SO_4\,(aq) + 2\,H^+\,(aq) + 2\,e^-, \quad E° = -0.158\text{ V}\\ &\text{Cathode: } 2\,H^+\,(aq) + 2\,e^- \rightarrow H_2\,(g), \quad E° = 0.0\text{ V}\\ &\text{Overall: } 2\,H_2O\,(l) + SO_2\,(aq) \rightarrow H_2SO_4\,(aq) + H_2\,(g), \quad E° = -0.158\text{ V}\end{aligned} \qquad (2)$$

is only −0.158 V[1,2] when the SO_2 is dissolved in pure H_2O. The Nernst equation can be used to show that the standard potential for SO_2-depolarized electrolysis in 50 wt% H_2SO_4 (a more likely anolyte) is about −0.26 V. Taking into account the combined effect of overpotentials, resistance, and other inefficiencies, the actual cell voltage for SO_2-depolarized electrolysis in aqueous H_2SO_4 anolyte should be about one-fourth to one-third that for commercial alkaline electrolysis.

Several different ways of carrying out the SO_2-depolarized electrolysis portion of the cycle are being investigated or have been proposed. Early conceptual flowsheets featured a single electrolysis step using recirculating H_2SO_4 anolyte and catholyte separated by a microporous diaphragm, with SO_2 dissolved in the anolyte under pressure to maximize concentration.[3] Bench-scale experiments confirmed the viability of this configuration.[4] As advancements in fuel cell technology led to improved proton exchange membrane (PEM) materials, PEM-based SO_2-depolarized electrolyzers (SDEs) have been proposed and are being investigated as well.[5] One SDE version currently under laboratory development uses recirculating H_2SO_4 anolyte containing dissolved SO_2 and no catholyte.[6] Moist H_2 is generated at the cathode. Another SDE version undergoing laboratory development feeds gaseous SO_2 to the anode, where concentrated H_2SO_4 is produced and removed, and liquid H_2O to the cathode, where H_2 bubbles form, accumulate, and are removed.[7] Conceptual flowsheets with a single electrolysis step have been proposed for both PEM SDE configurations. Flowsheets have also been proposed in which electrolysis is carried out in multiple steps at different conditions.[8]

These alternatives are being simulated on a common design basis using Aspen Plus™ software. Sensitivity analyses are helping determine the performance potential of each configuration, and the flowsheets are being optimized for energy recovery. Net thermal efficiencies are calculated for the best set of operating conditions for each flowsheet and the results compared. This will help focus attention on the most promising electrolysis alternatives. The sensitivity analyses should also help identify those changes that offer the greatest potential improvement.

II. METHODOLOGY

The analysis begins with a complete flowsheet and material and energy balance constructed for the specific SDE under consideration, using Aspen Plus™ software. A fixed H_2 production rate of 1-kmol/sec is assumed so that calculated heat transfer duties in units of kW are interchangeable with kJ/kmol H_2 or J/mol H_2 produced.

Aspen Plus™ was chosen as the basis for flowsheet models because of its flexibility, power, and universal acceptance. Since the credibility of a flowsheet model is largely determined by the validity of its underlying stream properties and phase equilibrium models, careful consideration was given to this aspect of the analysis.

Aspen Technology, Inc. (AspenTech) provides its licensees an oleum data package that can be inserted into Aspen Plus™ to provide accurate representation of H_2SO_4 properties and phase equilibria over the entire concentration range, from 0 through 100% H_2SO_4 to 100% sulfur trioxide (SO_3 or oleum). Unfortunately, the temperature range for this data package extends no higher than 150°C, while the pressure is limited to about 2 bar. This limitation was removed by Mathias in work commissioned by General Atomics for modeling the SI cycle.[9] (This is one example of how the HyS cycle has benefited from SI cycle development.) The results of Mathias' work are in the public domain.[10]

Mathias split his H_2SO_4 properties model into two temperature ranges. For "moderate" temperatures (below about 300°C), he simultaneously fit an adaptation of AspenTech's oleum model to the vapor-liquid equilibrium correlation developed by Gmitro and Vermeulen[11] and to excess enthalpy[12] and heat capacity[13] data for H_2SO_4-H_2O mixtures. This model makes use of the Chen Electrolyte-NRTL (ELECNRTL) property method in Aspen Plus™ and assumes that H_2SO_4 dissociates into ionic species. At higher temperatures (above 300°C), where the electrolyte model tends to break down, he switched to a complex-forming model, replacing the dissociation equilibria of H_2SO_4,

$$H_2SO_4\,(aq) + H_2O\,(l) \leftrightarrow H_3O^+ + HSO_4^-, \quad (3)$$
$$HSO_4^- + H_2O\,(l) \leftrightarrow H_3O^+ + SO_4^{2-}, \quad (4)$$

with a nonvolatile complex-forming equilibrium,

$$H_2SO_4\,(aq) + H_2O\,(l) \leftrightarrow 2\ \text{IonPair}. \quad (5)$$

Mathias fit this model to the high-temperature, high-pressure data of Wüster[14] as well as to extrapolations of the lower temperature excess enthalpy and heat capacity data. The following plot (Fig. 2), reproduced from Mathias' report[9], compares the high-temperature model predictions with Wüster's data. As can be seen there, the high-temperature H_2SO_4 properties model reproduces Wüster's data quite well.

The HyS flowsheet models use an adaptation of Mathias' H_2SO_4 properties method. An adjustment was made in the solubility of SO_2 in aqueous H_2SO_4 to take into account solubility data that was not considered by Mathias in his development. (SO_2 is treated as a HENRY_COMPS or supercritical component in most streams, except when the possibility of a separate, SO_2-rich liquid phase is high.) The optimal transition from the low-temperature, electrolyte to high-temperature, complex-forming model was found to occur at 270°C. (The smallest differences between enthalpies calculated using

the two methods for a given temperature, pressure, and composition were typically observed around 270°C.) Consequently, a switch from one properties method to the other is arbitrarily imposed whenever a stream crosses 270°C.

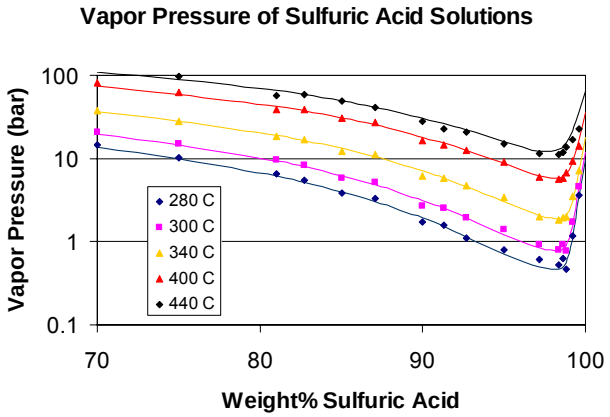

Fig. 2 Vapor Pressure of Sulfuric Acid Solutions at High Temperature – Comparison with Wüster[14] Data

Once the flowsheet is completed and converged, the stream heating and cooling data are extracted into the Aspen HX-Net heat integration application so that a pinch analysis[15] can be applied to optimize energy utilization. HX-Net automates the generation of composite heating and cooling curves and calculates the high-temperature nuclear heat target. It also provides both graphical and algorithmic methods for performing process optimization. These are used to adjust the temperatures of heat exchangers, condensers, reactors, and distillation columns, as well as the pressures of columns, pumps, throttling valves, and reactors in an effort to minimize the quantity of high-temperature nuclear heat required per unit of H_2 production.

Finally, the effect of uncertainties in the projected performance of the electrolyzer on the performance of the overall flowsheet is determined through sensitivity analyses.

III. APPLICATION TO SPECIFIC SDE CONFIGURATIONS

As stated in the introduction, this approach is being applied to several different SDE configurations and the flowsheets that have been developed for them. The first of these is the PEM SDE that uses recirculating H_2SO_4 anolyte containing dissolved SO_2 and has no catholyte. This is the SDE and the HyS Process that are being developed at the Savannah River National Laboratory (SRNL) for the U. S. Department of Energy's (DOE's) Nuclear Hydrogen Initiative (NHI).

III.A. SRNL Electrolyzer and Flowsheet

A simplified schematic diagram of the SRNL SDE is presented in Fig. 3 below. The SDE is a PEM device, in which recirculating anolyte provides the H_2O that keeps the membrane hydrated and in which H_2 gas is evolved at the cathode. There is no catholyte other than the H_2O that is transported from the anolyte across the membrane and wets the cathode; it may be transported in sufficient quantity to exit as a separate liquid phase along with a H_2O vapor-saturated gaseous H_2 phase.

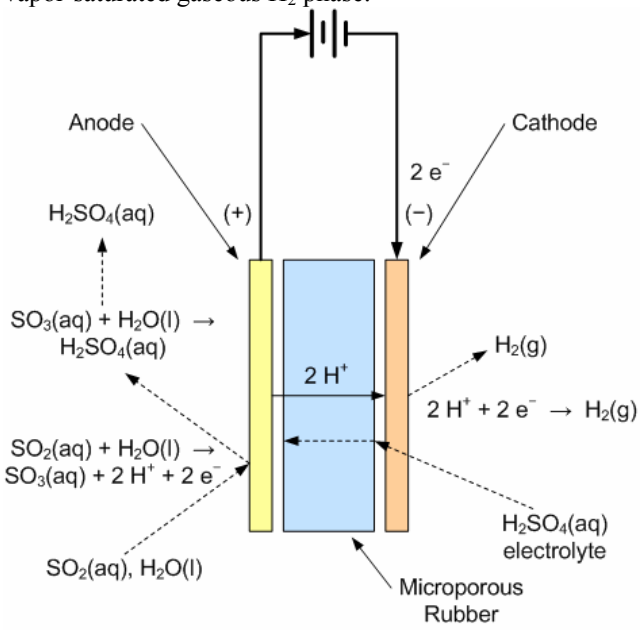

Fig. 3 SRNL SO_2-Depolarized Electrolyzer Configuration

At this stage of development, there is insufficient data to attempt a detailed design of the electrolyzers. Performance projections were made, instead, based on the results of ongoing experiments at SRNL[6] and on earlier work at Westinghouse with two-compartment, microporous diaphragm cells[16], and taking into account expected performance improvements. Based on this information, as well as on the feed stream and several input parameters (cell potential, current efficiency, SO_2 conversion, cell pressure drop, and molar H_2O-to-H^+ transport ratio), steady-state material and energy balances were used to calculate the product streams and two output parameters (electric power consumption and molar H_2 production rate).

The SRNL HyS flowsheet is shown in Fig. 4 below. Fresh anolyte (57.4 wt% H_2SO_4 at 21 bar and 80°C) enters the SDE (E-1) via stream 1. The electrolytic reaction (equation 2) takes place at a specified SO_2 conversion. Pressure drop across the anode half cell is specified as well. All of the H_2 made appears at the cathode and exits as product (stream 3) along with any H_2O transported across

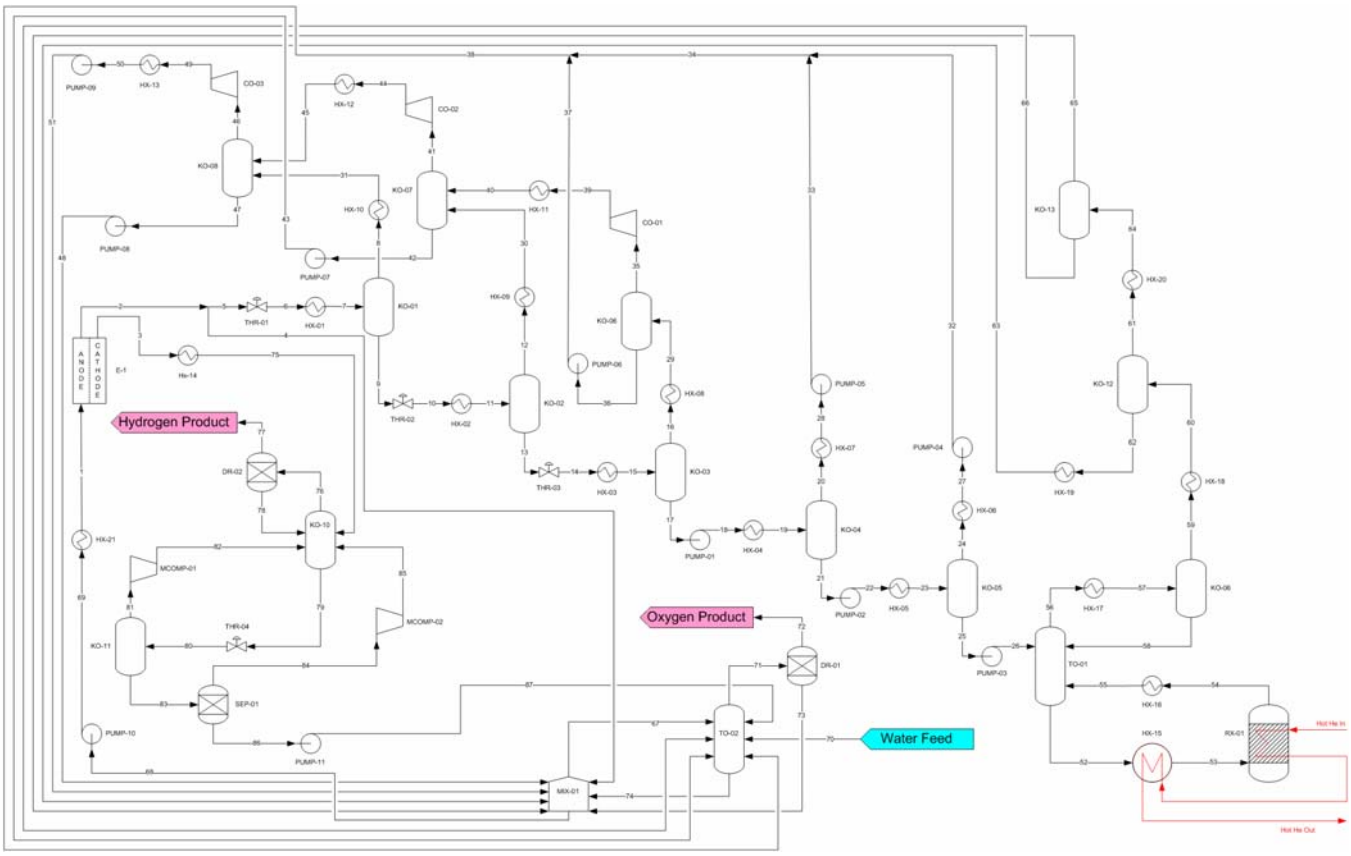

Fig. 4 SRNL HyS Process Flowsheet

the membrane by electro-osmotic drag[17] (assumed to be 3.5 mol H_2O/mol H^+, or 7 mol H_2O/mol H_2.) Everything else exits with the spent anolyte (stream 2).

The temperature rise across the electrolyzers due to voltage efficiency losses and ohmic heating is determined by an energy balance. The electric power required to produce the H_2 is calculated from the current efficiency, the cell voltage, and Faraday's constant. Anolyte effluent (and H_2 product) temperature (assumed to be identical) is then adjusted until the enthalpy difference between the product (2 and 3) and feed (1) streams matches the electric power input.

Table I below summarizes the performance characteristics that were used for the electrolyzers, and includes a comparison with earlier work at Westinghouse. A quick review confirms that, with respect to the previous flowsheets, all of the assumptions used for the current flowsheet are reasonable.

Returning to the process flow diagram (Fig. 4), streams 2 and 3 both exit the electrolyzer at 78.9°C and 20 bar. Wet H_2 product, consisting of a 7:1 molar ratio of H_2O and H_2, departs the cathode via stream 3, and is forwarded to the H_2/H_2O separation section. Spent anolyte (stream 2) is split into two streams. The smaller portion (stream 5) is passed on to H_2SO_4 concentration while the larger fraction (stream 4) is recycled to the anolyte prep tank (MIX-01). The flow split is set so that the molar production rate of H_2 is equal the amount of H_2SO_4 entering the decomposition loop (stream 26) minus the amount leaving through stream 59.

TABLE I

Electrolyzer performance summary and comparison

Header	1976 flowsheet	1983 flowsheet	SRNL flowsheet
Operating press., bar	25.86	20.0	20.0
Operating temp., °C	90.0	100.5	80.0
H_2SO_4 conc., wt%	66.3	63.0	65.0
SO_2 conc., wt%	7.7	10.8	8.95
SO_2 Conversion, %	47.2	2.2	50.0
Current efficiency, %	>99.0	100	99.0
Cell voltage, mV	450	607	525

The presence of H_2O in the cathode product requires that unit operations be added to separate a pure H_2 product stream from the H_2/H_2O mixture in stream 3. The first step is the cooling of stream 3 to 40°C using HX-14 (stream 75). Stream 75 is then adiabatically flashed in KO-10. The

liquid stream exiting KO-10, containing approximately 99.97 wt% H_2O, is depressurized through THR-04 (stream 80) to 1 bar and flashed adiabatically in KO-11. The vapor effluent from K0-11 (stream 81), with about 57.7 wt% H_2 is subsequently repressurized to 20 bar by means of a multi-stage compressor (MCOMP-01) and returned to KO-10. The liquid stream exiting KO-11 (stream 83) still contains a very small amount of H_2.

A generic separator (SEP-01) is used to recover the last of the H_2 into vapor stream 84. The mechanism by which the separator will operate has been left undetermined, but this should not be an issue because the quantity of H_2 involved is so small and its solubility in H_2O so low. The recovered H_2 (stream 84) is then pressurized to 20 bar using MCOMP-02 and returned to KO-10. The pure liquid H_2O effluent from SEP-01 (stream 86) is pressurized to 20 bar via PUMP-11 (stream 87) and sent to absorber TO-02 in the SO_2/O_2 separation section.

The vapor stream exiting KO-10 (stream 76) contains about 99.6 mol% H_2. The small fraction of H_2O remaining is removed by a dryer (DR-02). Liquid H_2O exiting DR-02 (stream 78) is recycled back to KO-10. The H_2 product stream exiting DR-02 (stream 77) contains 1 kmol/sec of pure H_2 at 40°C and 20 bar.

The H_2SO_4 concentration process is performed in five, sequential flash steps before the H_2SO_4 enters the high-temperature decomposition loop. Concentration begins with spent anolyte (stream 5), containing about 5.6 wt% SO_2 dissolved in 70 wt% H_2SO_4. The pressure of the spent anolyte is reduced through an adiabatic throttling device (THR-01) to 2.55 bar (Stream 6). Stream 6 is then heated in HX-01 (stream 7) to 120°C before being flashed in knock-out pot KO-01, vaporizing over 85% of the dissolved SO_2. The pressure of the liquid stream leaving KO-01 (stream 9) is reduced to 0.45 bar by THR-02 (stream 10), and then heated to 130°C by HX-02 (stream 11) before being flashed in KO-02. The pressure of the liquid stream exiting KO-02 (stream 13) is reduced still further to 0.086 bar by THR-03 (stream 14), heated to 145°C by HX-03 (stream 15), and then flashed in KO-03. These three steps produce a liquid stream (stream 17) which is about 83.6% H_2SO_4 by weight and contains less than 0.1 ppm SO_2.

The next step in the acid concentration section increases the pressure of stream 17 to 0.42 bar using PUMP-01 (stream 18), and heats it to 208°C in HX-04 (stream 19) before flashing the solution in KO-04. The resulting liquid (stream 21) is pressurized to 2.25 bar using PUMP-02 (stream 22), and heated to 280°C by HX-05 (stream 23) before the solution is flashed in KO-05. This results in the liquid stream 25 consisting of hot concentrated acid at 89% H_2SO_4 by weight.

PUMP-03 is used to pressurize the hot concentrated H_2SO_4 to 20 bar (stream 26), which is then fed to the top of the packed column (TO-01) in the high temperature H_2SO_4 decomposition loop.

TO-01 has twenty equilibrium stages and functions as a direct contact exchanger and SO_3/H_2SO_4 trap. Hot (280.6°C) concentrated acid (stream 26) is fed to the top, while partially cooled decomposition reactor effluent (stream 55), which consists of H_2O, H_2SO_4, SO_3, SO_2, and O_2 vapor at 394°C, is fed to the bottom. The vapor overhead (stream 56) removes H_2O but very little of the unreacted H_2SO_4 and SO_3. This results in an increased acid concentration (94.2%) in the bottoms (stream 52) at a temperature of 411.8°C.

The concentrated acid (stream 52) is circulated to HX-15 where it is vaporized and superheated to 700°C (stream 53) using a possible combination of hot helium secondary reactor coolant and interchange with stream 54. Stream 53 then enters the decomposition reactor (RX-01) where it is heated to a 900°C effluent temperature using hot helium secondary reactor coolant. The effluent from RX-01 (stream 54) is sent to HX-16 where it is cooled to 350°C and fed to the bottom of TO-01 (stream 55).

The vapor overhead of TO-01 (stream 56) is cooled to 235°C by HX-17 (stream 57). This causes a portion of the stream to condense. The liquid portion (stream 58) is separated in reflux drum KO-09, and only the vapor portion (stream 59) is withdrawn from the decomposition loop.

The H_2SO_4 concentration and decomposition operations produces various vapor streams that need to be condensed, combined (with all of the SO_2 dissolved in the liquid phase and all of the O_2 removed), and repressurized to 20 bar. Stream 59 is cooled to 100°C to condense roughly half of the stream. The solution is flashed in KO-12, to produce a liquid and vapor stream. The liquid (stream 62) is cooled to 40°C in HX-19, before being sent to MIX-01 via stream 63. The vapor effluent from KO-12 (stream 61) is cooled to 40°C in HX-20 (stream 64). Stream 64 is then flashed in KO-13 to produce a liquid (stream 66), and a vapor (stream 65). Stream 65 is sent to TO-02, while stream 66 is forwarded to MIX-01.

The effluent from KO-05 (stream 24) is cooled to 40°C by means of HX-06 and pressurized to 20 bar using PUMP-04 (stream 32). The effluent from KO-04 (stream 20) is cooled to 40°C in HX-07 and pressurized to 20 bar via PUMP-05 (stream 33). Streams 32 and 33 are combined to form stream 34.

The effluent from KO-03 (stream 16) is cooled to 40°C in HX-08 (stream 29), and flashed in KO-06. The liquid stream exiting KO-06 (stream 36) is compressed to 20 bar by means of PUMP-06 (stream 37). Stream 37 is combined with stream 34 and sent to TO-02. The vapor stream leaving KO-06 (stream 35) is compressed to 0.45 bar via CO-01 (stream 39) and cooled to 40°C using HX-11 (stream 40).

The effluent from KO-02 is cooled to 40°C in HX-09 (stream 30) and flashed in KO-07 along with stream 40. The liquid stream exiting KO-07 (stream 42) is pressurized to 20 bar by PUMP-07 (stream 43) and forwarded to TO-02. The vapor stream exiting KO-07 (stream 41) is compressed to 2.55 bar with CO-02 (stream 44), and cooled to 40°C in HX-12 (stream 45).

The effluent of KO-01 is cooled to 40°C by means of HX-10 (stream 31), and flashed in KO-08 along with stream 45. The resulting liquid (stream 47) is pressurized to 20 bar using PUMP-08 (stream 48) and sent to the MIX-01. The vapor stream leaving KO-08 (stream 46) is compressed by CO-03 to 12 bar (stream 49) and cooled to 40°C by HX-13 (stream 50), where it completely condenses. Stream 50 is then pressurized to 20 bar by PUMP-09 (stream 51), and sent to MIX-01.

TO-02, the SO_2 Absorber, is a twelve-stage packed column operating at 20 bar. The liquid streams 43, 38, and 70 are fed to TO-02 on different stages depending on SO_2 content to ensure optimal separation. Vapor streams 66 and 67 enter at the bottom of TO-02. The amount of makeup H_2O fed to TO-02 (stream 70) is set to equal the molar production rate of H_2 in E-1 (stream 3) to satisfy the material balance.

The SO_2-enriched bottoms from TO-02 (stream 74) is fed to the anolyte prep tank, MIX-01. The moist O_2 overhead from TO-02 (stream 71) is passed through DR-01, a drying/polishing bed that removes the remaining H_2O and trace SO_2 to produce a pure O_2 product (stream 72). Liquid H_2O and dissolved SO_2 removed by DR-01 are sent to MIX-01 via stream 73.

MIX-01 is the anolyte prep tank. The liquid streams 48, 51, 63, 65, 4, 74, and 73 are combined in MIX-01 to form the anolyte feed to the electrolyzer. Mixing of these streams results in a small vapor fraction that is sent to TO-02 via stream 67. The combined liquid anolyte (stream 68) is pressurized by PUMP-10 to 21 bar (stream 69) and cooled to 80°C by HX-21 (stream 1). Stream 1 is then fed back to the anolyte inlet of E-1.

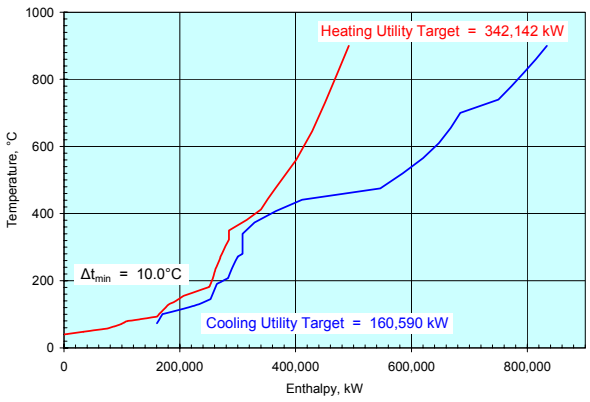

Fig. 5 SRNL HyS Flowsheet Composite Curves

The Aspen Plus™ simulation of this flowsheet was used to perform a pinch analysis with Aspen HX-Net. The resulting composite curves are shown in Fig. 5 above. Table II below summarizes the heat exchange requirements for a 1-kmol H_2/sec production rate, while Table III lists the work requirements, including the SDE electricity demand.

TABLE II

Heat Exchange Requirements for the SRNL HyS Flowsheet

Unit No.	Description	Duty, kW	Temperature, °C	
			Inlet	Outlet
HX-01	Heat Exchanger	16,364	73.0	120.0
HX-02	Heat Exchanger	5,823	116.9	130.0
HX-03	Heat Exchanger	70,257	100.6	145.0
HX-04	Heat Exchanger	30,264	145.0	208.0
HX-05LT	Heat Exchanger	16,557	208.1	270.0
HX-05HT	Heat Exchanger	8,352	272.0	280.0
HX-06HT	Heat Exchanger	533	280.0	270.0
HX-06LT	Heat Exchanger	9,698	266.0	40.0
HX-07	Heat Exchanger	13,497	208.0	40.0
HX-08	Heat Exchanger	58,847	145.0	40.0
HX-09	Heat Exchanger	2,108	130.0	40.0
HX-10	Heat Exchanger	795	120.0	40.0
HX-11	Heat Exchanger	171	214.4	40.0
HX-12	Heat Exchanger	280	194.4	40.0
HX-13	Heat Exchanger	3,836	174.2	40.0
HX-14	Heat Exchanger	22,419	78.9	40.0
HX-15A	Heat Exchanger	238,096	339.9	475.0
HX-15B	Heat Exchanger	137,856	475.0	700.0
HX-16A	Heat Exchanger	126,867	900.0	475.0
HX-16B	Heat Exchanger	80,037	475.0	350.0
HX-17HT	Heat Exchanger	14,428	322.5	270.0
HX-17LT	Heat Exchanger	7,316	267.8	235.0
HX-18	Heat Exchanger	81,582	236.0	100.0
HX-19	Heat Exchanger	7,702	100.0	40.0
HX-20	Heat Exchanger	20,944	100.0	40.0
HX-21	Heat Exchanger	40,645	93.4	80.0
RX-01	Decomp. Rxtr.	149,718	700.0	900.0
MComp-01/1	Intercoler 1	4.6	182.0	100.0
MComp-01/2	Intercoler 2	9.3	267.4	100.0
MComp-01/3	Intercoler 3	18.5	267.5	40.0
MComp-02/1	Intercoler 1	0.21	184.1	100.0
MComp-02/2	Intercoler 2	0.42	270.1	100.0
MComp-02/3	Intercoler 3	0.57	270.3	40.0

Using the heating utility target of 342.1 MJ/kmol H_2, and converting the total work requirement, 104.0 MJ_e/kmol H_2, to its thermal equivalent, 216.6 MJ_{th}/kmol H_2 (assuming that high-temperature nuclear heat is used to make electric power for the process at 48% efficiency with an advanced Brayton cycle Power Conversion Unit), the net thermal efficiency for hydrogen production is 51.1% on a higher heating value (HHV) basis. This provides a benchmark against which to measure the performance of other SDE configurations and flowsheet arrangements.

Table III

Shaft/Electrical Work Requirements for the SRNL HyS Flowsheet

Unit No.	Description	Work, kW	Temp., °C	
			Inlet	Outlet
CO-01	Compressor	25.11	40.0	214.4
CO-02	Compressor	139.4	40.3	194.4
CO-03	Compressor	733.5	40.3	174.5
MCOMP-01	Multi-stg. Comp.	26.52	40.4	40.0
MCOMP-02	Multi-stg. Comp.	1.21	40.4	40.0
E-01	SDE	102,333	80.0	78.9
PUMP-01	Pump	3.18	145.0	145.0
PUMP-02	Pump	17.42	208.0	208.1
PUMP-03	Pump	188.6	280.0	280.6
PUMP-04	Pump	13.38	40.0	40.7
PUMP-05	Pump	18.88	40.0	40.6
PUMP-06	Pump	66.12	40.0	40.3
PUMP-07	Pump	5.73	40.3	41.5
PUMP-08	Pump	1.36	40.3	41.5
PUMP-09	Pump	9.62	40.0	41.1
PUMP-10	Pump	107.1	93.4	93.4
PUMP-11	Pump	295.7	40.4	40.5

III.B. SRNL Electrolyzer Modifications

The SRNL flowsheet was based on the results of earlier work at Westinghouse (with an SDE that used a microporous diaphragm separator between the anode and cathode chambers[16]), taking into account the expected behavior of PEM-based SDEs. However, after more than two years of PEM-based SDE electrolyzer development work at SRNL,[6] it now appears that at least some of the assumptions used in building the flowsheet need to be revisited.

The most important of these is how high an H_2SO_4 concentration to maintain in the anolyte. Excess water must be removed prior to H_2SO_4 decomposition, increasing the overall heat requirement, so the higher the anolyte acid content, the higher the thermal efficiency of the decomposition process. The earlier (Westinghouse) work suggested H_2SO_4 concentrations up to 65 wt% could be used in the SDE. However, Nafion® membranes do not appear to work very well at such high acid levels. The H_2SO_4 concentration may actually need to be considerably less than 65 wt%. That could greatly reduce the thermal efficiency of the high-temperature decomposition process.

This trade-off between cell performance and H_2SO_4 decomposition thermal efficiency needs to be investigated with the flowsheet model because SDE requirements could conceivably dictate an acid concentration that would be impractical from the perspective of the decomposition process. Such a study is underway, and the results will be reported when they become available.

Other changes being evaluated include various ways of reducing or mitigating the effect of SO_2 cross-over from the anode to the cathode, and replacement of the high-temperature decomposition loop (units TO-01, HX-15, HX-16, and RX-01) with the new bayonet reactor design that is being developed for use in the SI process by Sandia National Laboratories (SNL).[18,19] SNL's high-temperature decomposition reactor design may help offset some of the loss in thermal efficiency caused by operating the SDE at lower H_2SO_4 concentrations because of its efficient energy recovery. Flowsheet models have been prepared and the effects of the proposed changes are being studied. Results will be reported as soon as the work is completed.

III.C. Other Electrolyzers and Flowsheets

Similar analyses are being prepared for two other electrolyzer configurations. One of these is the SDE design of Weidner and co-workers at the University of South Carolina (USC), illustrated in Fig. 6 below.

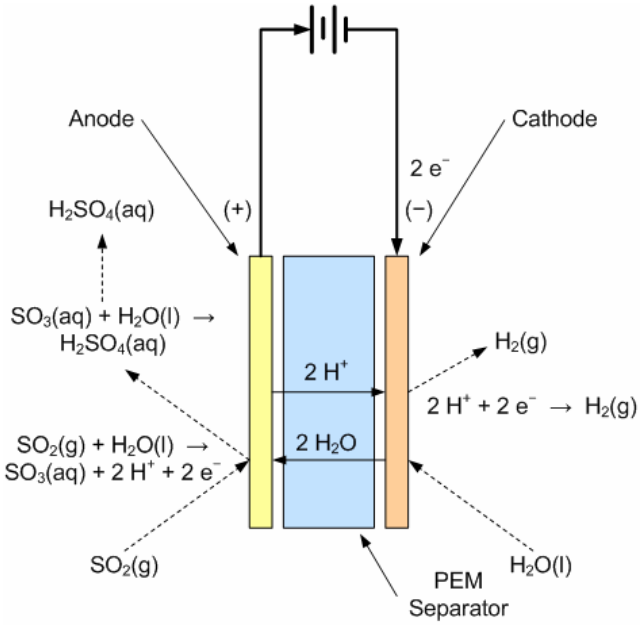

Fig. 6 USC SO_2-Depolarized Electrolyzer Configuration

The USC SDE feeds gaseous SO_2 to the anode and liquid H_2O to the cathode. H_2O diffuses across the PEM from the cathode to the anode, where it reacts with SO_2 to form concentrated H_2SO_4 product. The protons and electrons that are also produced recombine at the cathode where they form H_2 bubbles that accumulate and are withdrawn as product.

The flowsheet is similar to that used for the SRNL SDE with a few changes. The biggest difference is that the product of the high-temperature decomposition reaction is treated differently, so that a gaseous SO_2 stream can be fed to the anode.

The other SDE configuration is the staged electrolysis and SO_2 absorption concept proposed by Westinghouse Electric[8] (Fig. 7 below).

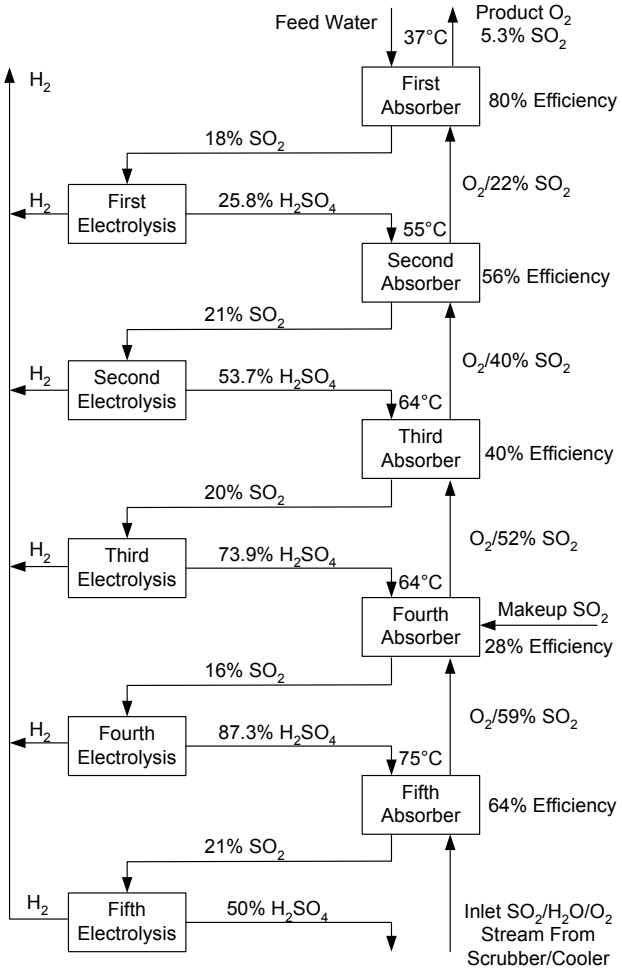

Fig. 7 Westinghouse Five-Stage SDE/SO_2 Absorber Design (reproduced from Ref. 8)

The flowsheet is presented in detail elsewhere.[8] It differs substantially from the SRNL flowsheet. SO_2 absorption is staged in conjunction with the SDE, and all five SDEs operate at very different conditions.

Both the USC and Westinghouse flowsheets are being modeled in Aspen Plus™ and analyzed with HX-Net, using the same bases and properties models as the SRNL process. The results will be reported when they become available.

IV. CONCLUSIONS

Several different ways of carrying out the SO2-depolarized electrolysis step in the HyS cycle have been proposed. These alternatives are being evaluated with complete flowsheet simulations and on a common design basis using Aspen Plus™. Sensitivity analyses are being performed to assess the performance potential of each configuration, and the flowsheets optimized for energy recovery. Net thermal efficiencies are being calculated for the best set of operating conditions for each flowsheet and the results compared. To date, the analysis has been completed only for the SRNL flowsheet, which should be capable of achieving 51.1% net thermal efficiency (HHV basis). The USC and Westinghouse flowsheets are being evaluated at this time, as are several modifications to the SRNL process. Results will be reported upon completion.

ACKNOWLEDGMENTS

This work is being performed by SRNL under DOE Contract No. DE-AC09-96SR18500. Funding is being provided by the DOE Office of Nuclear Energy, Science and Technology under the NHI and also under the Nuclear Energy Research Initiative. Mr. Carl Sink is the current technical program monitor. His support is acknowledged and greatly appreciated. The assistance of Mr. Jason A. Eargle and Prof. Travis W. Knight from USC is also gratefully acknowledged, as are helpful interactions with Dr. Paul M. Mathias (formerly with AspenTech, now with Fluor Corp.), Dr. David F. McLaughlin (Westinghouse Electric Co.), Dr. William A. Summers (SRNL), and Prof. John W. Weidner (USC).

NOMENCLATURE

AspenTech	Aspen Technology, Inc.
DOE	U. S. Department of Energy
ELECNRTL	Electrolyte-NRTL (properties method)
H_2	Hydrogen
H_2O	Water
H_2SO_4	Sulfuric acid
HHV	Higher heating value, 286 kJ/mol H_2[20]
HyS	Hybrid Sulfur
H^+	Hydrogen cation (proton)
NHI	Nuclear Hydrogen Initiative
O_2	Oxygen
PEM	Proton exchange membrane
SDE	SO_2-depolarized electrolyzer

SI	Sulfur-Iodine
SNL	Sandia National Laboratories
SO_2	Sulfur dioxide
SO_3	Sulfur trioxide
SRNL	Savannah River National Laboratory
USC	University of South Carolina
V	Volts

REFERENCES

1. S. G. Bratsch, "Standard Electrode Potentials and Temperature Coefficients in Water at 298.15K" *J. Phys. Chem. Ref. Data*, **18,** 1 (1989).

2. A. J. Bard, R. Parsons, and J. Jordan, eds., "Standard Potentials in Aqueous Solutions," Marcel Dekker, Inc., New York (1985).

3. G. H. Farbman, *The Conceptual Design of an Integrated Nuclear-Hydrogen Production Plant Using the Sulfur Cycle Water Decomposition System*, NASA Contractor Report, NASA-CR-134976, Washington, D. C. (1976).

4. P. W. T. Lu, E. R. Garcia, and R.L. Ammon, "Recent Developments in the Technology of Sulfur Dioxide Depolarized Electrolysis," *J. Appl. Electrochemistry*, **11,** 347 (1981).

5. W. A. Summers, M. B. Gorensek, and M. R. Buckner, "The Hybrid Sulfur Cycle for Nuclear Hydrogen Production," *Proc. of GLOBAL 2005*, paper 097, Tsukuba, Japan, Oct. 9-13 (2005).

6. J. L. Steimke and T. J. Steeper, "Generation of Hydrogen Using Electrolyzer with Sulfur Dioxide Depolarized Anode," paper 126c, 2006 AIChE Annual Meeting, San Francisco, Nov. 12-17 (2006).

7. J. W. Weidner, J. Staser, and P. Sivasubramanian, "Electrochemical Generation of Hydrogen via Thermochemical Cycles, " paper 126d, 2006 AIChE Annual Meeting, San Francisco, Nov. 12-17 (2006).

8. E. J. Lahoda, D. F. McLaughlin, P. R. Mulik, W. Kriel, R. Kuhr, C. O. Bolthrunis, and M. Corbett, "Estimated Costs for the Improved HyS Flowsheet," *Proc. HTR2006, 3rd Intern. Topical Mtg. on High Temp. Reactor Technol.*, Johannesburg, South Africa, October 1-4 (2006).

9. P. M. Mathias, "General Atomics and Sandia National Laboratories; Modeling the Sulfur-Iodine Cycle; Aspen Plus™ Building Blocks and Simulation Models," Final Report from Aspen Technology, Inc. to General Atomics, Oct. 24 (2002).

10. L. C. Brown et al., "High Efficiency Generation of Hydrogen Fuels Using Nuclear Power," Final Technical Report for the period August 1, 1999 through September 30, 2002, from General Atomics Corp. to US DOE, GA–A24285, Jun (2003), Appendix C.

11. J. I. Gmitro and T. Vermeulen, "Vapor-Liquid Equilibrium for Aqueous Sulfuric Acid," AIChE J., **10,** 740 (1964).

12. S. H. Kim and M. Roth, "Enthalpies of Dilution and Excess Molar Enthalpies of an Aqueous Solution of Sulfuric Acid," *J. Chem. Eng. Data*, **46,** 138 (2001).

13. O. T. Fasullo, "Sulfuric Acid: Use and Handling," McGraw-Hill, New York (1965).

14. G. Wüster, "p, v, T – und Dampfdruckmessungen zur Bestimmung Thermodynamischer Eigenschaften Starker Elektrolyte bei Erhöhtem Druck," doctoral dissertation, RWTH-Aachen (1979).

15. B. Linnhoff, D. W. Townsend, D. Boland, and G. F. Hewitt, "A User Guide on Process Integration for the Efficient Use of Energy," Institution of Chemical Engineers, IChemE, Houston, TX (1994).

16. P. W. T. Lu, R. L. Ammon, and G. H. Parker, *A study on the electrolysis of sulfur dioxide and water for the sulfur cycle hydrogen production process*, NASA Contractor Report, NASA-CR-163517, Washington, D. C. (1980).

17. T. A. Davis, J. D. Genders and D. Pletcher, "A First Course In Ion Permeable Membranes," The Electrochemical Consultancy, Romsey, England (1997).

18. F. Gelbard, R. C. Moore, M. E. Vernon, E. J. Parma, D. A. Rivera, H. B. J. Stone, J. C. Andazola, G. E. Naranjo, P. S. Pickard, "Sulfuric Acid Decomposition with Heat and Mass Recovery Using a Direct Contact Exchanger," paper 230b, 2006 AIChE Annual Meeting, San Francisco, Nov. 12-17 (2006).

19. H. B. J. Stone, M. E. Vernon, E. J. Parma, F. Gelbard, and R. C. Moore, "Heat Transfer within a Ceramic Heat Exchanger used for Sulfuric Acid

Decomposition," paper 480b, 2006 AIChE Annual Meeting, San Francisco, Nov. 12-17 (2006).

20. National Research Council, *The Hydrogen Economy: Opportunities, Costs, Barriers, and R&D Needs*, National Academies, Washington, DC (2004), p. 240.